SMC-TR-95-26

AEROSPACE REPORT NO.
TR-92(2925)-2

Steady State Field Pattern in a Multimode Semiconductor Laser Cavity

20 October 1993

Prepared by

H. SUHL
University of California, San Diego

F. L. VERNON, Jr. and W. R. FENNER
Electronics Technology Center
Technology Operations
The Aerospace Corporation

Prepared for

SPACE AND MISSILE SYSTEMS CENTER
AIR FORCE MATERIEL COMMAND
2430 E. El Segundo Boulevard
Los Angeles Air Force Base, CA 90245

Engineering and Technology Group

THE AEROSPACE CORPORATION
El Segundo, California

This report was submitted by The Aerospace Corporation, El Segundo, CA 90245-4691, under Contract No. F04701-88-C-0089 with the Space and Missile Systems Center, 2430 E. El Segundo Blvd., Los Angeles Air Force Base, CA 90245. It was reviewed and approved for The Aerospace Corporation by T. A. Galantowicz, Principal Director, Electronics Technology Center.

This report has been reviewed by the Public Affairs Office (PAS) and is releasable to the National Technical Information Service (NTIS). At NTIS, it will be available to the general public, including foreign nationals.

This technical report has been reviewed and is approved for publication. Publication of this report does not constitute Air Force approval of the report's findings or conclusions. It is published only for the exchange and stimulation of ideas.

Linda DeHainaut

Linda DeHainaut
SMC/PL/LIDA

REPORT DOCUMENTATION PAGE

Form Approved
OMB No. 0704-0188

1. AGENCY USE ONLY (*Leave blank*)	2. REPORT DATE	3. REPORT TYPE AND DATES COVERED
	20 October 1993	

4. TITLE AND SUBTITLE

Steady State Field Pattern in a Multimode Semiconductor Laser Cavity

5. FUNDING NUMBERS

F04701-88-C-0089

6. AUTHOR(S)

Suhl, Harry; Vernon, Jr., Frank L.; and Fenner, Wayne R.

7. PERFORMING ORGANIZATION NAME(S) AND ADDRESS(ES)

The Aerospace Corporation
Technology Operations
El Segundo, CA 90245-4691

8. PERFORMING ORGANIZATION REPORT NUMBER

TR-92(2925)-2

9. SPONSORING/MONITORING AGENCY NAME(S) AND ADDRESS(ES)

Space and Missile Systems Center
Los Angeles Air Force Base
Los Angeles, CA 90009-2960

10. SPONSORING/MONITORING AGENCY REPORT NUMBER

SMC-TR-95-26

11. SUPPLEMENTARY NOTES

12a. DISTRIBUTION/AVAILABILITY STATEMENT

Approved for public release; distribution unlimited

12b. DISTRIBUTION CODE

13. ABSTRACT (*Maximum 200 words*)

The competing effects of carrier recombination and diffusion are modeled for a simplified semiconductor laser cavity.

14. SUBJECT TERMS

Semiconductor laser, Laser diode, Spatial hole burning, Carrier recombination, Carrier diffusion

15. NUMBER OF PAGES

23

16. PRICE CODE

17. SECURITY CLASSIFICATION OF REPORT	18. SECURITY CLASSIFICATION OF THIS PAGE	19. SECURITY CLASSIFICATION OF ABSTRACT	20. LIMITATION OF ABSTRACT
UNCLASSIFIED	UNCLASSIFIED	UNCLASSIFIED	

Contents

Figures

I. Introduction

In all nonlinear oscillators, the growth of the amplitude of the oscillation is ultimately curbed by back reaction of the growing signal on the agent powering the oscillation. In the case of the semiconductor laser the back reaction consists in the increased recombination rate of the excess carriers responsible for the laser action. At any point in the device, the increase in recombination rate over its normal equilibrium value is proportional to the local power density of the laser field. This depletion of the carrier density diminishes the gain of the device, providing the negative feedback that ultimately stabilizes the laser output at a self-consistent operating level. Since to a good approximation the increase in recombination rate is a local effect, the excess carrier density profile will be nonuniform, reflecting the intensity distribution of the mode, but this non-uniformity is counteracted by carrier diffusion.

Thus one has a nonlinear problem to solve: Maxwell's equations with carrier density dependent dielectric constant, together with the diffusion equation with field intensity dependent recombination rate, and with a steady source term reflecting the carrier injection process in the form of an assigned current. One can go back further and trace that current back to a boundary value problem for the voltage distribution that sets up that current,[1] making extensive use of the computer. We stop short of this step since it is difficult to see how it can affect the results in a major way.

The method we use to "solve" the simultaneous nonlinear equations is conventional: the electric field satisfying Maxwell's equations with a complex dielectric constant (depending on carrier density) and the carrier density are expanded in a series of cavity modes, with amplitudes that are functions of time. Then the condition for a steady state is written down (in the steady

*H. Suhl is Professor of Physics at the University of California, San Diego. He was supported in this work by USAF Contract F04701-88-C-0089.

state, the electric field varies with time as a superposition of sinusoids, whereas, to a very good approximation, the carrier density is time independent). The steady state condition yields a sequence of recursion relations for the Fourier coefficients, which is broken off at an early stage. This is justified if the field-induced recombination rate (the ultimate source of the nonlinearity) is small compared with the equilibrium recombination rate.

There is a large body of literature on this subject.[3–6] Most of it addresses specific issues of diode laser operation. In this paper, we analyze only the most primitive "toy model" that still exhibits the spatial hole burning phenomenon in analytic (as distinct from purely computational) form.

II. Analysis

Let n denote the excess carrier density. We assume that the diffusion equation for n can be

$$\frac{\partial n}{\partial t} = \frac{J}{\delta} + D\nabla^2 n - \frac{n}{\tau} - 2\alpha\overline{F^2}n \tag{1}$$

where J is the driving current (in general a function of position), δ is the thickness of the active layer, α is a coupling constant to the electromagnetic field and D is the diffusion coefficient. (The sign of J is as shown, because carriers are being generated by it.) $\overline{F^2}$ is the time averaged square of the total electromagnetic field (time averaged, because the carrier concentration is unlikely to follow variations at optical frequencies). If n were the *total* carrier density, Eq. (1) would have to include higher powers of n inasmuch as the recombination process is bimolecular and possibly also has an Auger component that is cubic in n.[2] However, if n is regarded as the excess carrier density needed to push the system over the threshold to its operating point, and that excess is not too great, equation (1) is adequate. To begin with, consider a cavity consisting of two infinite parallel plates a distance a apart, with the E-field polarized *parallel* to the plates. For this polarization direction, and in the absence of injected carriers, there can be resonances at a series of frequencies: the lowest is at $\omega = \pi/(a\sqrt{\epsilon_0\mu})$, and the higher ones are integral multiples thereof. Here ϵ_0 is the real part of the dielectric constant of the unactivated medium. In the presence of the non-

linearity implied by the last term in Eq. (1), the steady state cannot involve one single mode alone. We shall restrict the argument to a superposition of two modes. In the presence of the current J, the dielectric constant becomes $\epsilon_{1,2} = \epsilon_0 + [\beta n + i(\gamma_0 - \gamma_{1,2} n)] \equiv \epsilon' + i\epsilon''$, to first order in the excess carrier concentration n. Here γ_0 denotes the intrinsic loss in the cavity, and $\gamma_{1,2}$ the gains in the two modes, per unit carrier concentration. For simplicity we assume that the real part of the dielectric constant is the same for both modes. The equation for the E-field for each mode is

$$\frac{\partial^2 E}{\partial z^2} = \frac{\epsilon \mu \partial^2 E}{\partial t^2},$$

where z is the distance across the cavity. For real ϵ it has a solution of the form $F(z)e^{i\omega t}$. When ϵ is complex, but its imaginary part is not too large, the solution has the form $F(z,t)e^{i\omega t}$, where F can be chosen real, and where the rate of variation of F is slow compared with ω, that is $(1/F)dF/dt \ll \omega$. Then we have two equations (F being real):

$$\frac{\partial^2 F}{\partial z^2} = -\omega^2 \epsilon' \mu F - \omega^2 \epsilon'' \mu \frac{\partial F}{\partial t} \tag{2a}$$

$$\epsilon' \frac{\partial F}{\partial t} + \omega \epsilon'' F = 0 \tag{2b}$$

where the second time derivative of F has been neglected. Substituting (2b) into (2a) gives an equation for the z-variation of F

$$\frac{\partial^2 F}{\partial z^2} + \omega^2 \left(\epsilon' + \frac{\epsilon''^2}{\epsilon'} \right) F = 0.$$

However, (2b) has a solution that decays or grows indefinitely depending on the sign of ϵ''. To determine a steady state, proceed as follows: Take the complete steady state of the field to have the form

$$E = F_1 \sin\left(\frac{\pi z}{a}\right) e^{i\omega t} + F_2 \sin\left(\frac{2\pi z}{a}\right) e^{2i\omega t}$$

and from now on measure distance in units of a/π, defining $\zeta = \pi z/a$. The dielectric constant depends on E. Evidently a steady state would be possible if $\epsilon''(E) \cdot E = 0$, for each of the two modes. Two equations for the amplitudes F_1 and F_2 are then obtained by using trigonometric identities to segregate out terms that go like $\sin(\pi z/a) \exp i\omega t$ and like

$\sin(2\pi z/a)\exp(2i\omega t)$ and equating them to zero separately. The first step is to express ϵ'' in terms of a solution of Eq. (1).

Equation (1), in the present one-dimensional case is, in the steady state,

$$\begin{aligned} -J' &= \frac{-n}{\tau} + D'\frac{d^2n}{d\zeta^2} - \alpha\overline{F^2}n \\ &= \frac{-n}{\tau} + D'\frac{d^2n}{d\zeta^2} - \alpha[F_1^2\sin^2\zeta + F_2^2\sin^2 2\zeta]n \end{aligned} \tag{3}$$

where $D' = D\pi^2/a^2$ and $J' = J/\delta$.

From this, and from the fact that $\sin^2\theta = (1/2)(1-\cos 2\theta)$, it is apparent that a consistent steady state is reached if it is assumed that n is a Fourier cosine series of the variable $2\pi z/a$:

$$n = n_0 + n_1\cos 2\zeta + n_2\cos 4\zeta + \ldots$$

We substitute this into (3), use sum and difference formulae for the cosine functions, and equate coefficients of the resulting trigonometric functions. This gives

$$\begin{aligned} J'\tau &= [1+\tau\alpha(F_1^2+F_2^2)]n_0 - \frac{1}{2}\tau\alpha F_1^2 n_1 - \frac{1}{2}\tau\alpha F_2^2 n_2 \\ 0 &= -\tau\alpha F_1^2 n_0 + \left[1 + 4\tau D' + \tau\alpha\left(F_1^2 + \frac{1}{2}F_2^2\right)\right]n_1 - \frac{1}{2}\tau\alpha F_1^2 n_2 \\ 0 &= -\tau\alpha F_2^2 n_0 - \frac{1}{2}\tau\alpha F_1^2 n_1 + \left[1 + 16\tau D' + \tau\alpha\left(\frac{1}{2}F_1^2 + F_2^2\right)\right]n_2. \end{aligned} \tag{4}$$

In this process, the sum formulae also generate $\cos 6\zeta$ terms, but these are discarded. They could be taken into account by including them in the ansatz for n. Continuing in this manner, one would eventually establish the full Fourier series for n. Hopefully this converges sufficiently rapidly so that the first few terms suffice.

Equations (4) are three simultaneous linear equations for n_0, n_1, n_2, which may be solved in terms of F_1^2 and F_2^2. If the nonradiative recombination rate is fast compared with the induced rate, then $\tau\alpha F^2$ is small, and an approximate solution to first order in $\tau\alpha F^2$ should suffice:

$$\begin{aligned} n_0 &= J'\tau(1-A-B) \\ n_1 &= \frac{An_0}{(1+4\tau D')} \end{aligned}$$

$$n_2 = \frac{Bn_0}{(1+16\tau D')} \tag{5}$$

where we have set

$$A = \tau\alpha F_1^2$$

$$B = \tau\alpha F_2^2.$$

Turning now to the steady state requirement $\epsilon'' E = 0$, mode by mode, we need

$$\begin{aligned} n\sin\zeta &= (n_0 + n_1\cos 2\zeta + n_2\cos 4\zeta + \ldots)\sin\zeta \\ &= \left(n_0 - \frac{1}{2}n_1\right)\sin\zeta + \text{terms in } \sin 3\zeta \text{ etc.} \end{aligned}$$

and similarly

$$n\sin 2\zeta = \left(n_0 - \frac{1}{2}n_2\right)\sin 2\zeta + \ldots.$$

So the steady state equations are

$$\begin{aligned} \gamma_0 - \gamma_1\left(n_0 - \frac{1}{2}n_1\right) &= 0 \\ \gamma_0 - \gamma_2\left(n_0 - \frac{1}{2}n_2\right) &= 0 \end{aligned}$$

or, from (5),

$$\begin{aligned} g_1 &= [q_1 A + B] \\ g_2 &= [A + q_2 B] \end{aligned} \tag{6}$$

where

$$g_{1,2} = \left[\frac{1-\gamma_0}{(\tau J\gamma_{1,2})}\right]$$

are assumed positive (i.e. gain rather than loss) and

$$q_1 = 1 + \frac{1}{2}(1+4\tau D')^{-1}, \qquad q_2 = 1 + \frac{1}{2}(1+16\tau D')^{-1} \quad .$$

Equation (6) may be solved for A and B:

$$\begin{aligned} A &= \frac{q_2 g_1 - g_2}{q_1 q_2 - 1} \\ B &= \frac{q_1 g_2 - g_1}{q_1 q_2 - 1}. \end{aligned} \tag{7}$$

This solution, based on the approximate solution (5) of Eq. (4), breaks down when the two inequalities, $q_1 g_1 > g_2$ and $q_2 g_2 > g_1$, are inconsistent. Evidently, they are consistent as long as $q_1 q_2 > 1$. For example, with $4\tau D'' \approx 1$, we have both q's approximately equal to two, so that the inequalities are satisfied.

The energy density at position ζ is

$$W = A \sin^2 \zeta + B \sin^2 2\zeta.$$

Figure 2(a) shows W for equal gains in the two modes, as a function of ζ and of $r = 4\tau D'$, which is effectively the ratio of recombination time to the time needed to diffuse through about one wavelength of the lower mode. Figures 3 and 4 show the results for unequal gains, as indicated in the captions. Figures 5 through 7 show corresponding carrier density variations.

III. Generalization to More Realistic Structures

Consider the geometry of Fig. 8 representing a one-stripe laser diode. A very similar procedure may be used in this case in which the current J, and therefore the dielectric constant is a function of x. We change that variable to $\xi = x\pi/a$. The diffusion equation is then

$$-\tau J'(\xi) = -n + D' \left(\frac{\partial^2 n}{\partial \xi^2} + \frac{\partial^2 n}{\partial \zeta^2} \right) - 2\alpha \tau^2 \overline{E^2} n \tag{8}$$

and we write

$$n = n_0(\xi) + n_1(\xi) \sin \zeta + n_2(\xi) \sin 2\zeta + \ldots. \tag{9}$$

The equation for the E-field is

$$\frac{\partial^2 E}{\partial \xi^2} + \frac{\partial^2 E}{\partial \zeta^2} - \eta(\xi, \zeta) \frac{\partial^2 E}{\partial t^2} = + \left(\frac{\epsilon_0 \mu a^2}{\pi^2 c^2} \right) \frac{\partial^2 E}{\partial t^2}. \tag{10}$$

Here ϵ_0 is the background dielectric constant, and

$$\eta(\xi, \zeta) = \left(\frac{\mu a^2}{\pi^2 c^2} \right) [(\beta - i\gamma_{1,2}) n(\xi, \zeta) + i\gamma_0]$$

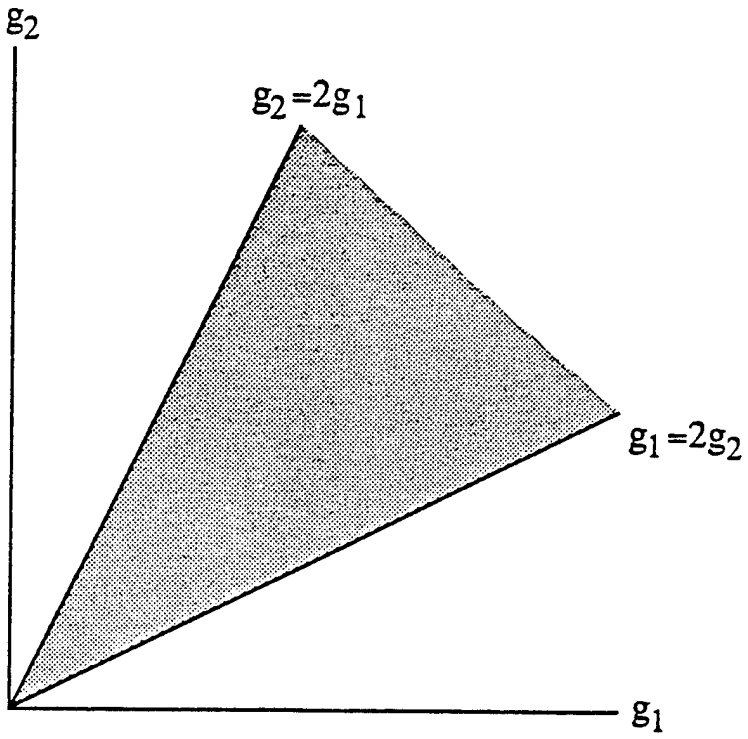

Fig. 1 In the shaded region of the $g_1 - g_2$ plane, the simple theory (non-radiative recombination rate $\gg$ radiative rate) applies.

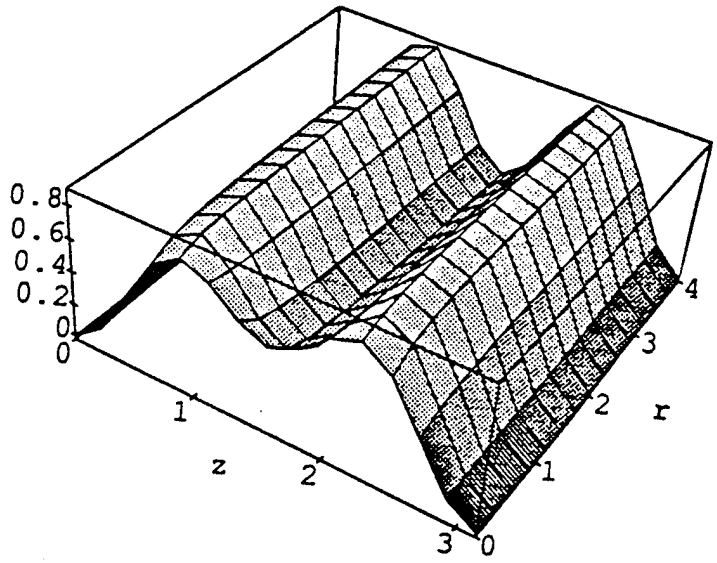

(a)

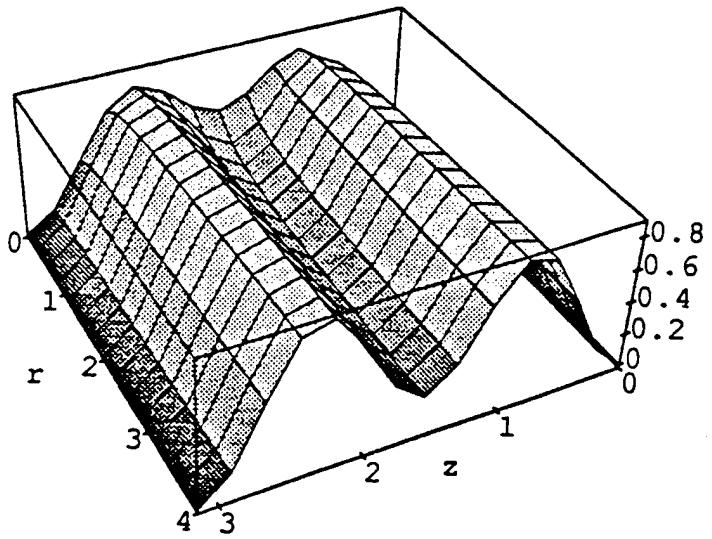

(b)

Fig. 2 Total energy density in the two lowest modes of a parallel plate cavity, as a function of distance z across the cavity and of r, the ratio of recombination time to the time needed to diffuse through roughly one wavelength. Here the two modes have equal gain, and are always in the shaded region of Fig. 1 no matter how large r: (a) view from the side $r < 0$. (b) view from large r.

(a)

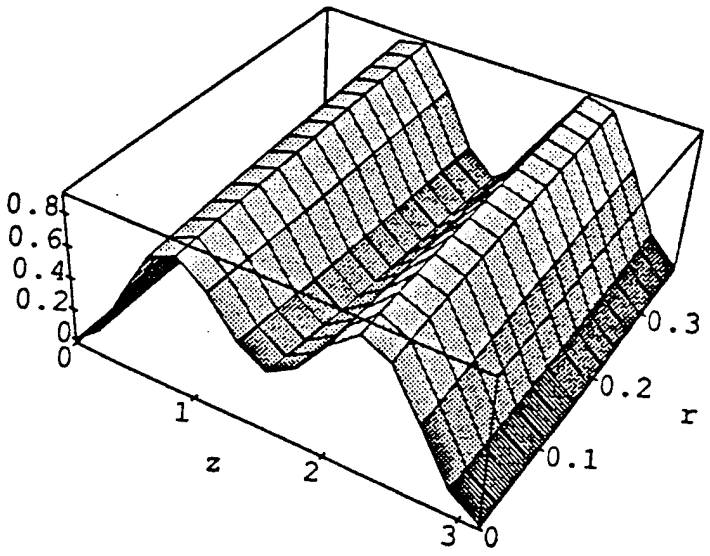

(b)

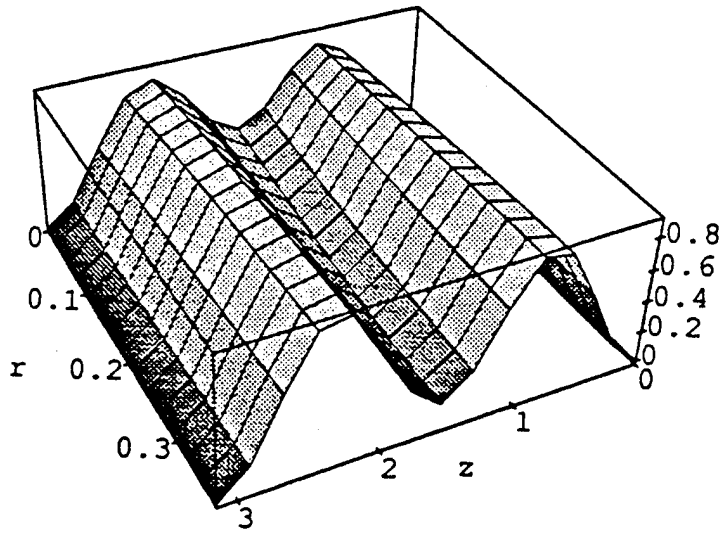

Fig. 3 As in Fig. 2, but with gain g_2 in higher frequency mode 1.2 times g_1. Maximum r allowed in the simple theory is now .375. (a) and (b) views from $r < 0$ and from $r > .375$.

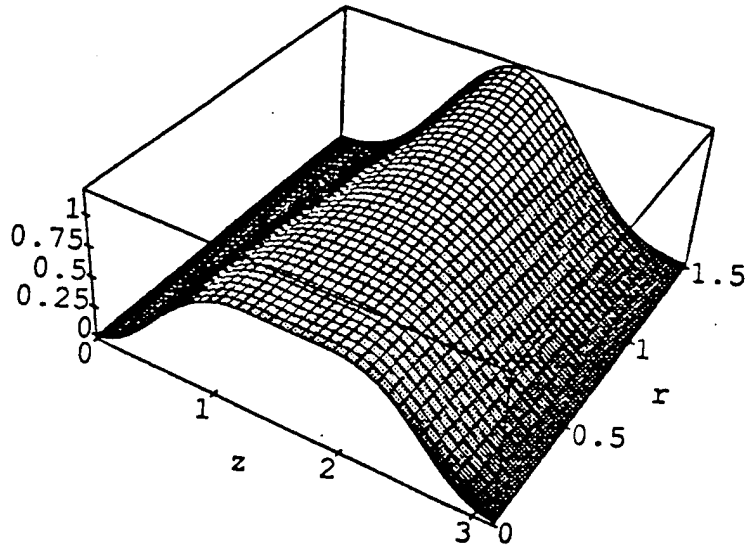

(a)

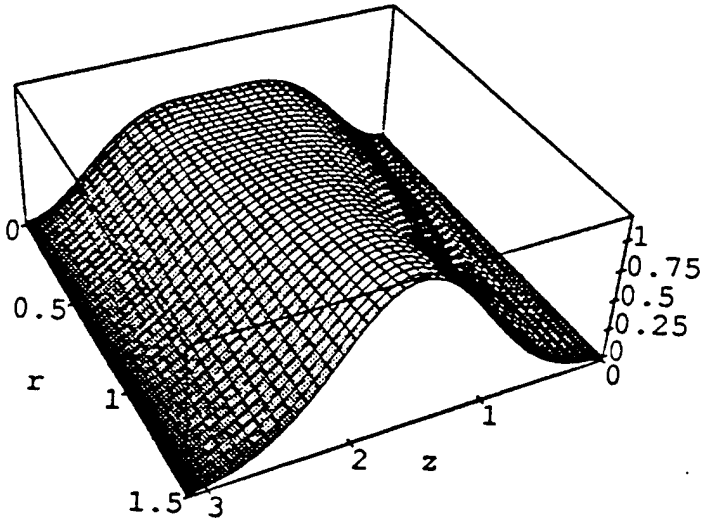

(b)

Fig. 4 $g_2 = .8g_1$. Maximum permitted r value =1.5. [(a) and (b) give the two views as in the preceding figures.]

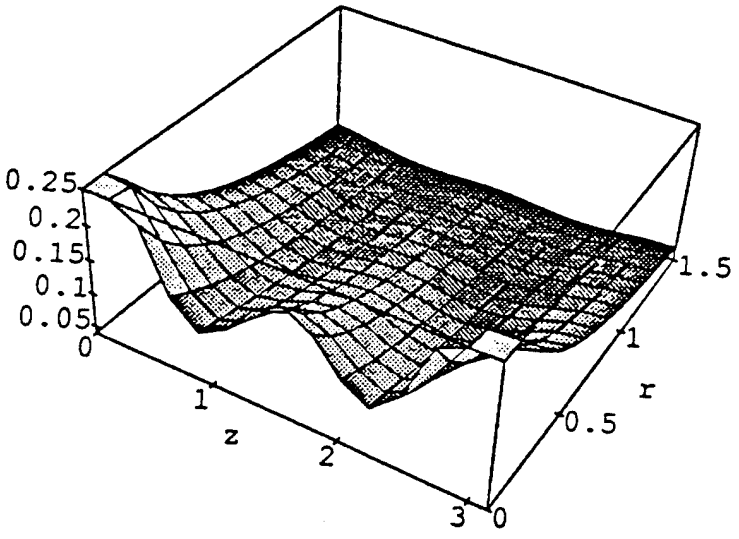

Fig. 5 Carrier density versus z and r in the parallel-plate cavity. $g_1 = g_2$.

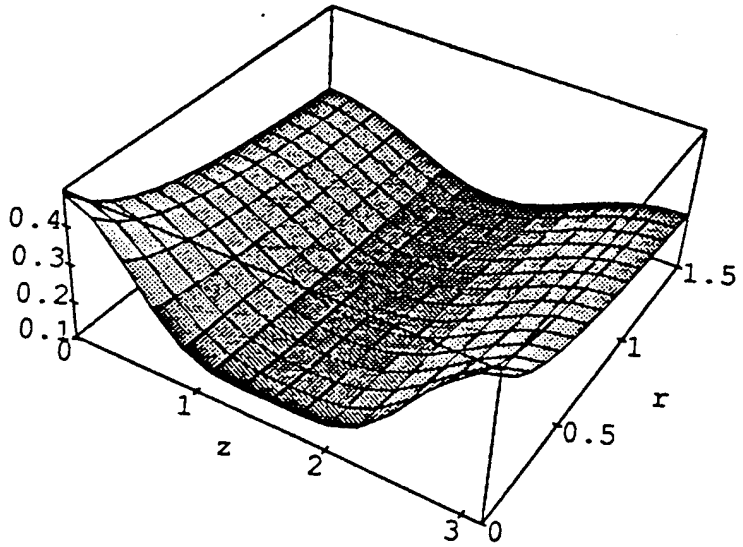

Fig. 6 Same as Fig. 10 but with $g_1 = 1$, $g_2 = .8$.

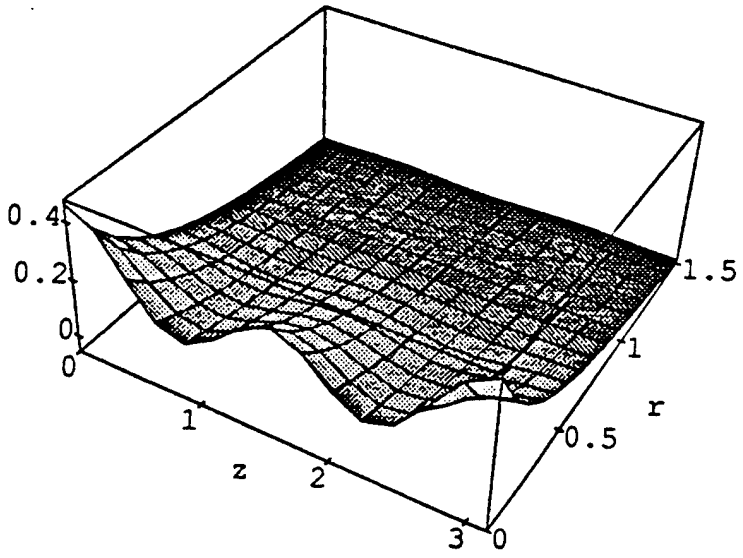

(a)

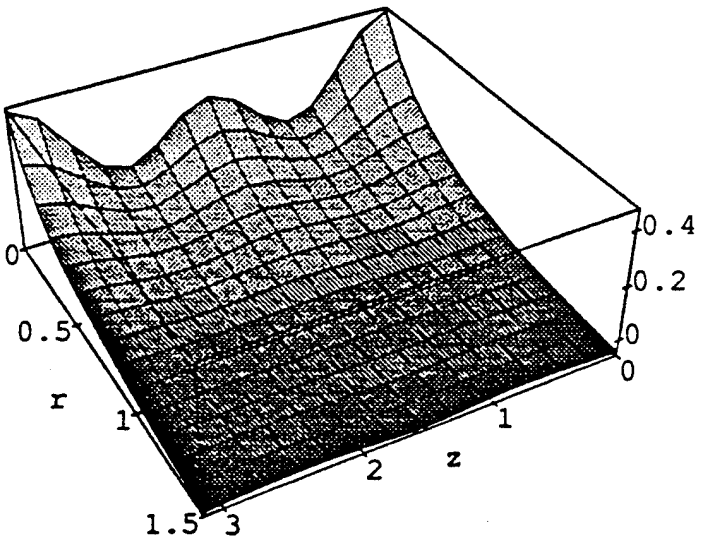

(b)

Fig. 7 Same as Fig. 10, but with $g_1 = 1$, $g_2 = 1.2$. (a) and (b) are front and rear views. Note that the maximum r for which n is still positive is larger (up to $r = 1.5$) than the maximum (.375) allowed to ensure positive squared field amplitudes. The latter figure of course governs.

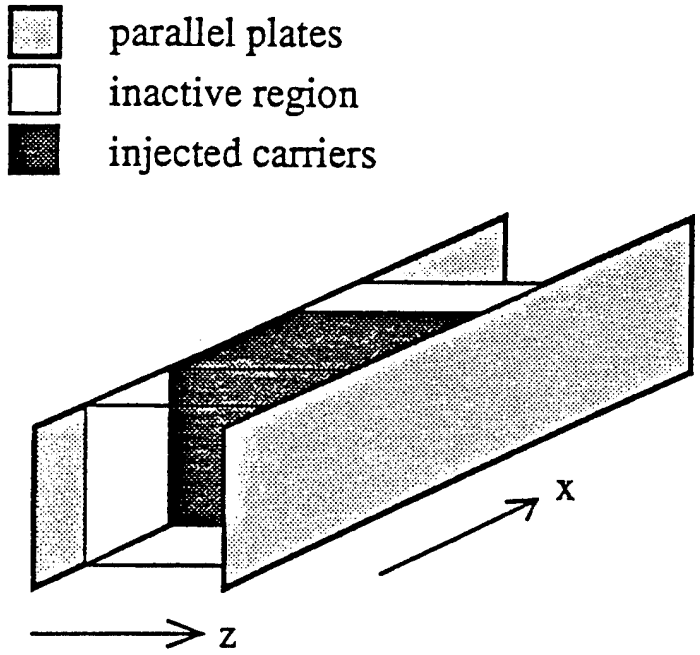

Fig. 8 Coordinate system for a one-stripe laser diode.

is the localized deviation from ϵ_0 induced by the carrier density. For the steady state, we assume a solution of (10) in the form

$$E = e^{i\omega_1 t} f_1(\xi) \sin\zeta + e^{i\omega_2 t} f_2(\xi) \sin 2\zeta,$$

where ω_1 and ω_2 will differ slightly from $\omega_0 = c\pi/(a\sqrt{\epsilon_0\mu})$ and $2\omega_0$. In the linear limit, i.e well below threshold, the functions $f_1(\xi)$ and $f_2(\xi)$ describe the transverse variations of two characteristic modes of the structure that go with the z variations $\sin\xi$ and $\sin 2\xi$, respectively. Here we shall discuss only two possibilities: (a) f_1 = lowest mode even in ξ; f_2 = lowest mode odd in ξ; (b) both f_1 and f_2 lowest even modes. In exactly the same way as for the parallel plate cavity, we find

$$nE = \left(n_0 - \frac{1}{2}n_1\right) f_1 e^{i\omega_1 t} \sin\zeta + \left(n_0 - \frac{1}{2}n_2\right) f_2 e^{i\omega_2 t} \sin 2\zeta + \cdots$$

where f_1 and f_2 satisfy

$$\begin{aligned}
\frac{\partial^2 f_1}{\partial\xi^2} + \left[(\beta - i\gamma_1)\left(n_0 - \frac{1}{2}n_1\right) - i\gamma_0\right]\left(\frac{\omega_1^2}{\omega_0^2}\right) f_1 &= \left[1 - \left(\frac{\omega_1}{\omega_0}\right)^2\right] f_1 \\
\frac{\partial^2 f_2}{\partial\xi^2} + \left[(\beta - i\gamma_2)\left(n_0 - \frac{1}{2}n_1\right) - i\gamma_0\right]\left(\frac{\omega_2^2}{\omega_0^2}\right) f_2 &= \left[4 - \left(\frac{\omega_2}{\omega_0}\right)^2\right] f_2 \qquad (11)
\end{aligned}$$

Also, substituting (9) in (8), we find

$$\begin{aligned}
\tau J'(\xi) &= \left[1 + \alpha\tau(f_1^2 + f_2^2) - \tau D'\frac{\partial^2}{\partial\xi^2}\right] n_0 - \frac{1}{2}\alpha\tau f_1^2 n_1 - \frac{1}{2}\alpha\tau f_2^2 n_2 \\
0 &= -\alpha\tau f_1^2 n_0 + \left[1 + \alpha\tau\left(f_1^2 + \frac{1}{2}f_2^2\right) + 4\tau D' - \tau D'\frac{\partial^2}{\partial\xi^2}\right] n_1 - \frac{1}{2}\alpha\tau f_2^2 n_2 \\
0 &= -\alpha\tau f_2^2 n_0 - \frac{1}{2}\alpha\tau f_1^2 n_1 + \left[1 + \alpha\tau\left(\frac{1}{2}f_1^2 + f_2^2\right) + 16\tau D' - \tau D'\frac{\partial^2}{\partial\xi^2}\right] n_2. \qquad (12)
\end{aligned}$$

As before, we discuss these equations for nonradiative recombination time short compared with radiative recombination time, i.e. $\alpha\tau f_{1,2}^2 \ll 1$. Then the field terms in Eq. (12) can be dropped, except where they compete with the diffusion term, i.e. inside the square parentheses. There they could be important for multistripe lasers. If we were to drop *all* field dependent terms, the equation for n_0 would be

$$\tau J'(\xi) = n_0 - \tau D'\frac{\partial^2 n_0}{\partial\xi^2}$$

whose solution is

$$n_0 \approx \int d\xi' J'(\xi') \exp\left(\frac{-|\xi - \xi'|}{\sqrt{D'\tau}}\right)$$

and the exponential tends to fuzz the edges of the current profile. So if two stripes are less than a distance $\sqrt{D'\tau}\times$ a wavelength apart, they would tend to act like a single stripe. If the field terms are retained in the parenthesis, they will have (very roughly) the effect of replacing τ by $\tau/[1 + \tau\alpha \times$ an average of $(f_1^2 + f_2^2)]$. It is plausible to suppose that this is the most sensitive spot at which the fields affect the carrier concentration, and so we shall disregard terms in higher powers of $\tau\alpha f^2$ everywhere except this place.

We begin by considering this problem for $D' = 0$. Then in the same approximation as for the parallel plate problem

$$\begin{aligned} n_0 &= \tau J'(\xi)[1 - \alpha\tau(f_1^2 + f_2^2)] \\ n_1 &= \alpha\tau f_1^2 n_0 = \alpha\tau^2 J'(\xi) f_1^2 \\ n_2 &= \alpha\tau f_2^2 n_0 = \alpha\tau^2 J'(\xi) f_2^2 \end{aligned} \tag{13}$$

to first order in $\alpha\tau f^2$. Equations (11) now become

$$\begin{aligned} \frac{\partial^2 f_1}{\partial\xi^2} + \left[(\beta - i\gamma_1)\tau J'(\xi)\left(1 - \frac{3}{2}\alpha\tau f_1^2 - \alpha\tau f_2^2\right)\right]\left(\frac{\omega_1^2}{\omega_0^2}\right) f_1 &= \sigma_1 f_1 \\ \frac{\partial^2 f_2}{\partial\xi^2} + \left[(\beta - i\gamma_1)\tau J'(\xi)\left(1 - \alpha\tau f_1^2 - \frac{3}{2}\alpha\tau f_2^2\right)\right]\left(\frac{\omega_2^2}{\omega_0^2}\right) f_2 &= \sigma_2 f_2 \end{aligned} \tag{14}$$

where $\sigma_{1,2} = -(1 + i\gamma_0)(\omega_{1,2}/\omega_0)^2$. We "solve" these in a manner similar to that for the parallel plates, except that we have here no comparably convenient sum and difference formulae for the eigenfunctions of the $J'(\xi)$ potential. Let $\psi_{0,1}(x)$ be the lowest and next to lowest eigenfunctions of that potential, satisfying

$$\frac{d^2\psi_{0,1}}{d\xi^2} + \left(\frac{\omega_1^2}{\omega_0^2}\right)\beta\tau J'(\xi)\psi_{0,1} = \lambda_{0,1}\psi_{0,1}$$

and going to zero at $\xi = \pm\infty$.

Suppose that J' is an even function of ξ. Then the eigenfunctions are either even or odd about $\xi = 0$, and the lowest one is even, the next to lowest is odd. Assume, with case

(a),

$$f_1(\xi) = p\psi_0(\xi) + \text{terms in higher even eigenfunctions}$$

$$f_2(\xi) = q\psi_1(\xi) + \text{terms in higher odd eigenfunctions} \tag{15}$$

where p and q are constants. Next we expand f_1^3 etc. in a series of even eigenfunctions, and keep only the first term. If the eigenfunctions are normalized

$$J'(\xi)\{f_1(\xi)\}^3 = p^3 h_{11}\psi_0(\xi) + \ldots; \quad J'(\xi)\{f_2(\xi)\}^2 f_1(\xi) = pq^2 h_{21}\psi_0(\xi)$$

$$J'(\xi)\{f_2(\xi)\}^3 = q^3 h_{22}\psi_1(\xi) + \ldots; \quad J'(\xi)\{f_1(\xi)\}^2 f_2(\xi) = p^2 q h_{12}\psi_1(\xi), \tag{16}$$

where

$$h_{11} = J'_m \int j\psi_0^4 d\xi, \quad h_{21} = J'_m \int j\psi_1^2\psi_0^2 d\xi = h_{12}, \quad h_{22} = J'_m \int j\psi_1^4 d\xi$$

and where $J'(\xi) = J'_m j(\xi)$, and J_m is the maximum in the current distribution. We further write

$$J'(\xi) f_{1,2}(\xi) = p g_{1,2}\psi_1(\xi), \text{ where } g_{1,2} = \int J'\psi_{1,2}^2 d\xi.$$

The condition for a steady state is that the imaginary part of the potential term should vanish in both Eqs. (11). This gives

$$\left[\frac{3}{2}h_{11}P + h_{12}Q\right] = g_1 - \frac{\gamma_0}{\gamma_1 \alpha\tau J'_m} \equiv G_1$$

$$\left[h_{12}P + \frac{3}{2}h_{22}Q\right] = g_2 - \frac{\gamma_0}{\gamma_1 \alpha\tau J'_m} \equiv G_2 \tag{17}$$

where $P = 1/2\ \alpha\tau p^2$ etc. These may be solved for P and Q and presumably give very similar behavior with respect to the transverse dimension that we had for the longitudinal dimension in the parallel plate case. We have

$$P = \frac{\left(\frac{3}{2}h_{22}G_1 - h_{12}G_2\right)}{\Delta}$$

$$Q = \frac{\left(\frac{3}{2}h_{11}G_2 - h_{12}G_1\right)}{\Delta} \tag{18}$$

with $\Delta = (9/4)h_{11}h_{22} - h_{12}^2$ which is always positive.

We now include diffusion. We note that the operator $d^2/d\xi^2$ does not change the parity of a wavefunction. We may consistently assume that n_0, n_1, n_2 expand in even eigenfunctions, and we assume that the lowest of these, ψ_0, dominates. (This is a little different from the ζ-dependence : In the ζ direction the densities persist right to the end plates, whereas in $\pm\xi$ directions the n's fall off to zero, like J'. So in the ζ direction we needed functions that were finite at the endpoints, the cosines in this case.) This means that a term such as $D'd^2n_{0,1}/d\xi^2$ may be replaced by $n_{0,1,2}D'\int d\xi\psi_1 d^2\psi_1/d\xi^2 \equiv -\overline{D}n_{0,1,2}$, where $\overline{D}$ is *positive* because the curvature of ψ_1 is negative The only effect this would have on Eqs. (13) is to replace τ by $\tau/(1+\tau\overline{D})$ everywhere. As far as diffusion in the ξ-direction is concerned, the solution (18) therefore remains intact, except for that replacement in the definitions of P, Q, and the G's. However, diffusion in the ζ direction is another matter. Just as in the case of the parallel plates, it has the effect of replacing the factor 3/2 in the first of Eq. (18) by q_2, and in the second of (18) by q_1.

To plot the energy density in the cavity as a function of ξ and ζ we need the two lowest eigenfunctions. Suppose that $J'(\xi)$ has a $\mathrm{sech}^2\xi$ variation. This has the advantage that the exact eigenfunctions are known.[7] We write $(\omega_1^2/\omega_0^2)\tau J'(x) = \eta_{1,2}\mathrm{sech}^2\xi$. The lowest eigenvalue is

$$\lambda_0 = \left(\eta_1 + \frac{1}{4}\right)^{1/2} - \frac{1}{2}$$

and the corresponding (unnormalized) eigenfunction is

$$\psi_0 = (\mathrm{sech}\xi)^{\epsilon_0}.$$

The next one has

$$\lambda_1 = \left(\eta_2 + \frac{1}{4}\right)^{1/2} - \frac{3}{2}$$

with

$$\begin{aligned}\psi_1 &= \sinh\xi(\mathrm{sech}\xi)^{\epsilon_1+1} \\ &= \sinh\xi\psi_0\end{aligned}$$

it being assumed that η is large enough to support this mode. For convenience, chose $\eta = 15/4$. Then $\lambda_0 = 3/2$ and $\lambda_1 = 1/2$. Then numerical evaluation gives $h_{11} = 5\pi/32$.

$h_{12} \approx h_{22} = \pi/32$, $g_1 = 2/3$, $g_2 = 1/3$. The local energy density is

$$W = P\text{sech}^3\xi \sin^2\zeta + Q \sinh^2\xi \text{sech}^3\xi \sin^2 2\zeta. \tag{19}$$

Figures 9 through 11 show various cases, with f_1 and f_2 the lowest modes of opposite parity. Figures 12 and 13 refer to the case of f_1 and f_2 both of even parity.

When r becomes too large (which effectively causes the field induced recombination rate to dominate), this simple theory dependent on the convergence of a mode expansion breaks down. This does not necessarily mean that no steady state exists. If it does exist, nonperturbative solutions for the steady state must be sought.

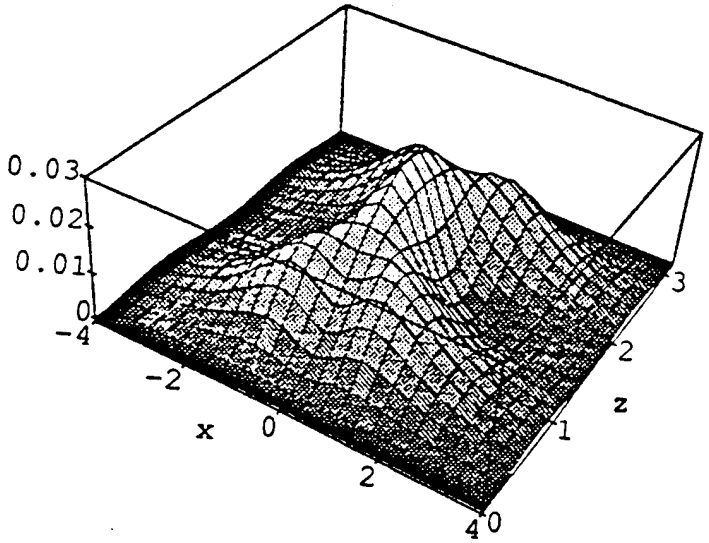

Fig. 9 Energy distribution with f_1 even, f_2 odd, in a single stripe structure. Energy density versus x (dimension transverse to the stripe), and z. Here $G_1 = 3G_2$ and $r = 0$. (In the text, this implies that the γ's must be different for the two modes, otherwise the relation between G_1 and G_2 would be predetermined. Thus for $\gamma_0 = 0$ in both modes we would have $G_1 = 2G_2$).

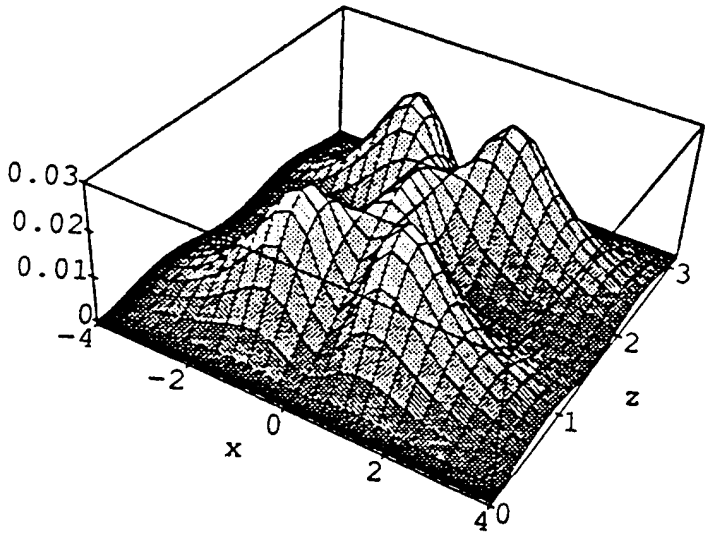

Fig. 10 As in Fig. 5, but with $G_1 = 2G_2$ and $r = 0$.

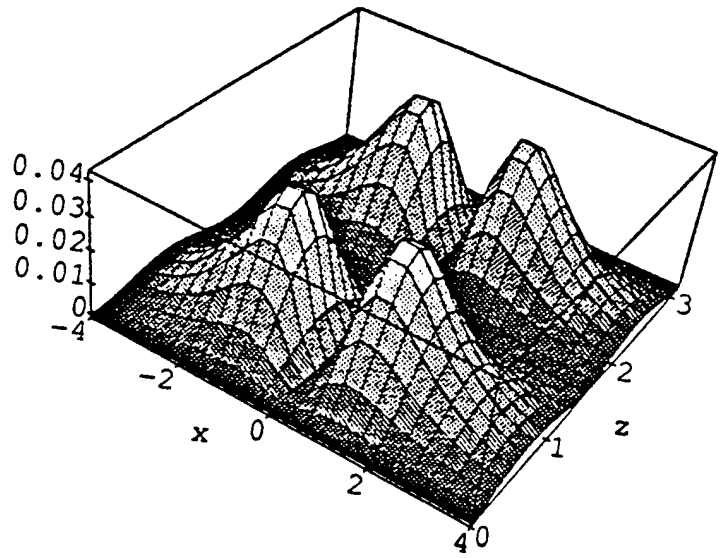

Fig. 11 As in Fig. 5, but with $G_1 = G_2$, and $r = 5$. The reason why the holeburning here is generally more marked than in the parallel plate cavity is that the important overlap integrals of the two modes with each other and with the current distribution are different.

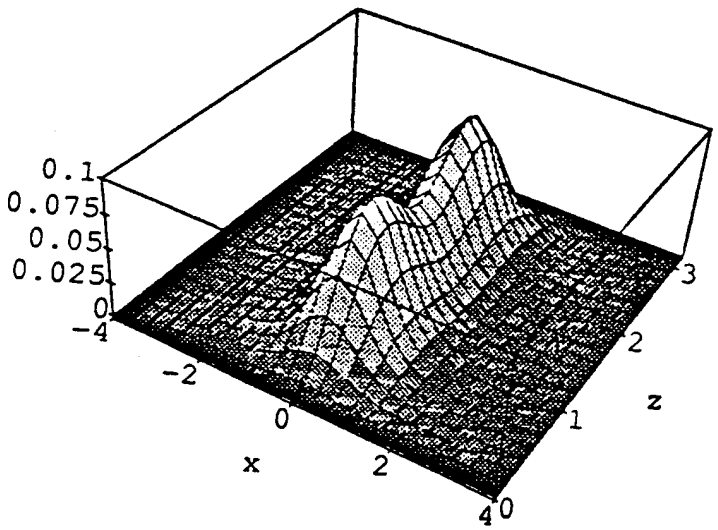

Fig. 12 f_1 and f_2 both the lowest even modes for the single stripe case, for equal gains and $r = 0$.

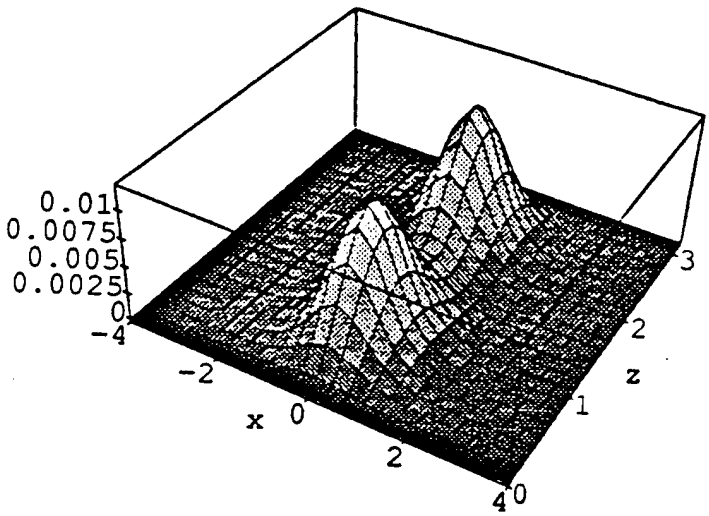

Fig. 13 Same as Fig. 12, but with $r = 5$.

References

1. KUMAR, ORMONDROYD and ROZZI, IEEE J. of Quantum Electronics **QE-21**, 421 (1985)

2. P.A. MORTON, R.F. ORMONDROYD and M.S. DEMOKAN, IEEE J. Quantum Electronics **QE-25**, 1559 (1989).

3. I.P. VAKWIKELBERGE, F. BUYTAERT, A. FRANCHOIS, R. BARETS, P.I. KUINDORSMA and C.W. FREDVIKSZ, IEEE J. Quantum Electronics **QE-25**, 2239 (1989).

4. KUO-LING CHEN and SHYH WANG , Applied Physics Letters **47**, 555 (1985).

5. D.P. WILT and AMMON YARIV, IEEE J. Quantum Electronics **QE-17**, 1941 (1981).

6. J. BUUS. IEEE J. Quantum Electronics **QE-24**. 22 (1988).

7. P. M. MORSE AND H. FESHBACH, Methods of Theoretical Physics, McGraw-Hill Book Company, Inc. (1953).

TECHNOLOGY OPERATIONS

The Aerospace Corporation functions as an "architect-engineer" for national security programs, specializing in advanced military space systems. The Corporation's Technology Operations supports the effective and timely development and operation of national security systems through scientific research and the application of advanced technology. Vital to the success of the Corporation is the technical staff's wide-ranging expertise and its ability to stay abreast of new technological developments and program support issues associated with rapidly evolving space systems. Contributing capabilities are provided by these individual Technology Centers:

Electronics Technology Center: Microelectronics, solid-state device physics, VLSI reliability, compound semiconductors, radiation hardening, data storage technologies, infrared detector devices and testing; electro-optics, quantum electronics, solid-state lasers, optical propagation and communications; cw and pulsed chemical laser development, optical resonators, beam control, atmospheric propagation, and laser effects and countermeasures; atomic frequency standards, applied laser spectroscopy, laser chemistry, laser optoelectronics, phase conjugation and coherent imaging, solar cell physics, battery electrochemistry, battery testing and evaluation.

Mechanics and Materials Technology Center: Evaluation and characterization of new materials: metals, alloys, ceramics, polymers and their composites, and new forms of carbon; development and analysis of thin films and deposition techniques; nondestructive evaluation, component failure analysis and reliability; fracture mechanics and stress corrosion; development and evaluation of hardened components; analysis and evaluation of materials at cryogenic and elevated temperatures; launch vehicle and reentry fluid mechanics, heat transfer and flight dynamics; chemical and electric propulsion; spacecraft structural mechanics, spacecraft survivability and vulnerability assessment; contamination, thermal and structural control; high temperature thermomechanics, gas kinetics and radiation; lubrication and surface phenomena.

Space and Environment Technology Center: Magnetospheric, auroral and cosmic ray physics, wave-particle interactions, magnetospheric plasma waves; atmospheric and ionospheric physics, density and composition of the upper atmosphere, remote sensing using atmospheric radiation; solar physics, infrared astronomy, infrared signature analysis; effects of solar activity, magnetic storms and nuclear explosions on the earth's atmosphere, ionosphere and magnetosphere; effects of electromagnetic and particulate radiations on space systems; space instrumentation; propellant chemistry, chemical dynamics, environmental chemistry, trace detection; atmospheric chemical reactions, atmospheric optics, light scattering, state-specific chemical reactions and radiative signatures of missile plumes, and sensor out-of-field-of-view rejection.